PTP TURBO BLANKETS

Report – Performance, No. 1   April 25, 2014

Performance Improvements of Turbocharged Engines with the Use of a PTP Turbo Blanket

by

Steffen Bickle, Graduate Research Assistant

Ronald D. Matthews, Professor of Mechanical Engineering
Head: Engines and Automotive Research Program

Engines Research Program, Thermal/Fluid Systems
Mechanical Engineering Department
Cockrell School of Engineering
The University of Texas at Austin

Table of Contents

THE UNIVERSITY OF TEXAS AT AUSTIN
WHAT STARTS HERE CHANGES THE WORLD

Nomenclature and Abbreviations

Abbreviations

CO_2	Carbon dioxide
ECM/ECU	Engine control unit, engine control module (used interchangeably)
EGR	Exhaust gas recirculation
EHR	Exhaust heat recovery
RPM, rpm	Revolutions per minute
SAE	Society of Automotive Engineers
TB	Turbo blanket
TC	Turbocharger
TH	Turbine Housing
Tu	Turbine
VGT	Variable geometry turbocharger

Variables

bp	Brake power
$bsfc$	Brake-specific fuel consumption
CF_a	Correction factor
CI	Confidence interval
D	Displacement
f	Correction coefficient, SAE J1349
fm	Mechanical engine factor
MAP	Absolute manifold pressure
$mean$	Arithmetic mean value
$\dot{m}_F$	Fuel mass flow rate
N	Number of cylinders
n	number of data points
P	Pressure
P_i^T	Barometric pressure
q	Variable in SAE J1349
rp	Intake pressure ratio
S	Viscosity sensitivity coefficient
SEM	Standard error of the mean, standard uncertainty of the mean
sg	Specific gravity

T	Temperature
T_2, T_2	Air temperature at compressor exit, boost temperature
T_3, T_3	Exhaust gas temp. at turbine inlet
T_4, T_4	Exhaust gas temp. at turbine exit
$T\_TC\text{-}exit\text{-}Oil$	Oil temp. at center section exit
$T\_Tu\text{-}exit\text{-}surf$	Exhaust pipe surface temperature at turbine exit
$T\_TH\text{-}surf\text{-}side$	Surface temperature on a side location of the turbine housing
$T\_TH\text{-}surf\text{-}top$	Surface temperature on top of the turbine housing
α	Factor in SAE J1349
β	Factor in SAE J1349
μ	Dynamic viscosity
ρ	Density of the fluid
σ	Standard deviation
τ	Torque
Ω	Relative humidity

Superscripts

c	Corrected
m	Measured
v	Vapor

Subscripts

a	Air
act	Actual
d	Density
f	Fuel
i	Intake
ref	Reference
sat	Saturation
v	Viscosity

List of Figures

Abstract

Efforts in R&D of modern vehicles are highly focused on improvements of the overall efficiency. The engine still has potential for better performance which not only implies pure efficiency considerations but also the power output specific to the engine size and weight. Turbochargers are a key technology. However, a significant amount of exhaust energy is lost through the turbine housing, and thus cannot be utilized to boost the intake air. If a certain portion of the lost heat can be conserved, however, the process in the turbine can be shifted more towards adiabatic expansion which, in theory, is the ideal case.

The Engines Research Program at The University of Texas at Austin conducted comparison tests of a PTP turbo blanket. The baseline engine was a Cummins 6.7 Turbocharged Diesel Engine hooked up to a Superflow SF-901 dynamometer. A series of steady-state points were obtained as well as three instantaneous load tip-in scenarios (hard acceleration transients) in order to test for changes in transient response due to the turbo blanket. In addition to seven thermocouples that we installed around the turbine we used the open ECU software to log a set of about 30 engine parameters.

The recorded data was first analysed with respect to the performance of the turbocharger alone. On the steady-state cases, the temperature increase of the turbine housing was significant while we did not measure a major increase of the oil temperature in the exit of the center section. According to these findings, oil "coking" was not a concern since the temperature difference of the oil with and without the turbo blanket was negligibly small. The boost pressure increase corresponded well with the higher turbo shaft speeds when the turbo blanket was applied.

Second, tip-in transients were performed to examine the difference in performance during a hard acceleration. The turbo spooled up more rapidly with the turbo blanket installed in comparison to the baseline configuration. In all cases this resulted in an improved boost performance in the intake and a significant time-to-torque advantage of the engine with a torque benefit of up to 140 Nm while the acceleration was improved by 200-250 rpm for most of the tip-in event.

This report presents detailed data regarding experiments in which the turbocharger and the engine are treated as an integrated system with a PTP turbo blanket applied in comparison to the baseline configuration for which the turbine housing is not insulated.

1   Introduction

Modern engines still work based on the same thermodynamic principles as their progenitors from the beginning of the combustion engine era (1876). However, their complexity has tremendously increased ever since. No other kind of vehicle has made such an impact on mankind as automobiles. Ongoing demands for higher mobility and individualism are the driving forces behind the huge worldwide car population. Due to the increasing sales in the 20th century, pollutant emissions from road vehicles became a major impact on the cleanliness of the ambient air. Therefore, emissions standards were established and applied over the years in more and more countries. Nowadays, our cars have reached emissions that are only a tiny fraction of the first standards enacted back in the 1960s. The R&D efforts by the automotive industry have changed in recent years; while still having to work to meet increasingly stringent emissions standards, the race is now governed by global warming effects which call for rapid improvements in fuel economy in order to reduce greenhouse gas emissions (CO_2).

The technology used in today's vehicles is already well advanced but will have to improve much more in order to reach the fuel economy goals set for the near future. Everything is under consideration, such as drivetrain efficiency, aerodynamics, kinetic energy recovery, and exhaust waste heat recovery. Car manufacturers have recently started to reduce the weight despite the fact that new vehicles will likely always carry more weight due to added technology in order to serve demands for safety, comfort, emissions, and so forth. Thus, the overall engine performance must be further improved. By increasing the specific power output we can make the engine smaller in order to match the initial power output and reduce the fuel consumption thereby. This is known as engine "downsizing". Bearing in mind that today's engines are already well advanced pieces of technology, we can conclude that the future vehicle will require even more advanced engine technology than today's vehicles.

It is safe to say that all modern compression ignition (Diesel) engines work with some sort of pressure boosting device, most often a turbocharger. The spark ignition (gasoline) engine has experienced a vast alteration in the last 10-15 years due to direct injection technology which, in turn, gave rise for rejuvenated turbocharger technology to come along with it. Within the next ten years or so, naturally aspirated engines will mostly have

disappeared from the markets and practically every non-electric passenger car will be driven with a boosted engine, most likely with a turbocharger.

Turbochargers mechanically connect the exhaust stream with the intake system so that exhaust energy is transferred to aid in engine aspiration. The energy (thermal and kinetic) contained in the hot exhaust gas leaving the combustion chamber can in this way be utilized to get more fresh charge into the cylinders during the intake process. Most of the exhaust energy is thermal energy which can be recuperated by the expansion process in the turbine of the turbocharger. However, due to the big temperature difference of the hot turbine surface and the surrounding air – which can be in the order of several hundred degrees Celsius – a significant portion of the exhaust energy is lost during the expansion process through the turbine section and, thus, cannot be gained as work for the compressor to boost the intake air.

In theory a perfectly insulated turbine would allow for adiabatic expansion. An adiabatic expansion process extracts the most possible work from the hot exhaust gas to drive the turbine wheel. However, in practice it is not possible to have perfect insulation. Thus, it is important to find a proper material to keep more thermal energy inside the turbine housing to produce increased turbine work, which transfers rotational mechanical energy over to the compressor resulting in higher intake manifold pressures. In this way, the turbocharger efficiency also increases.

The objective of the ongoing research is to investigate the potential benefits that might be derived from insulating the turbine section of a turbocharger using a PTP Turbo Blanket. This report presents the findings when the turbocharger and the engine are treated as an integrated system with a PTP Turbo Blanket[1] applied in comparison to the baseline configuration for which the turbine housing is not insulated. We primarily show how the boost performance of the turbocharger compares and what this means in terms of the torque output of the engine. Furthermore, we briefly discuss additional benefits that can mostly be derived from the fact that the turbo blanket significantly reduces the temperature influence on other engine parts in its vicinity.

---

[1] PTP Turbo Solutions, LLC., Austin TX; Supplier of turbo blankets and heat wraps; www.ptpturboblankets.com

2   Setup and Test Procedure

2.1 Test Cell Setup

Tests were conducted on a Cummins 6.7 L in-line 6-cylinder engine with a variable geometry turbocharger (VGT). The engine is a 2008 model with common rail injection operating with pilot, main, and post injection pulses for combustion control. We have open access to the engine control module (ECM) through an interface provided by Cummins. The engine is connected to an engine dynamometer (dyno) from SuperFlow, model SF-901. It is a water brake dyno with a "pressure boost" option that allows for higher torque absorption in the low speed range in comparison to the standard SF-901. However, the torque envelope does not enclose the entire speed-torque output range of the 6.7 L turbocharged Cummins engine. At 1600 rpm, the engine has a full load torque of τ = 1017 Nm (750 ft-lbf). However, at this speed the maximum allowable torque the dyno can absorb is approximately 300 Nm. Like most dynos, the SF-901 can be operated, via a control switch, in either speed (rpm) control or "load" (torque) control mode. If speed control is selected, the dyno will hold the rpm constant at the user's setpoint independent of what the operator does with the "accelerator pedal", the EGR rate, the fuel injection timing, etc. Similarly, if load control is selected, the dyno will hold the torque constant at the user's setpoint independent of what the operator does with the "accelerator pedal", the EGR rate, the fuel injection timing, etc. However, the dyno also has a "tip-in" switch. This allows a hard acceleration transient, but the transient will be either variable torque at constant rpm or variable speed at constant torque, depending upon whether the dyno is in speed or load control mode.

Figure 2-1 shows the cylinder head area with the valve covers on top and the turbocharger in the foreground. The turbocharger was equipped with seven thermocouples. Specific locations at and near the turbine give more insight into gas and component temperatures. This allowed for more in-depth analysis of thermodynamic states and also helps to evaluate temperature gradients resulting from internal and external surface temperature differences.   Moreover, we could compare the oil temperatures of the turbocharger center section and also obtain an estimate of the temperature effects on parts in the vicinity of the hot turbine.
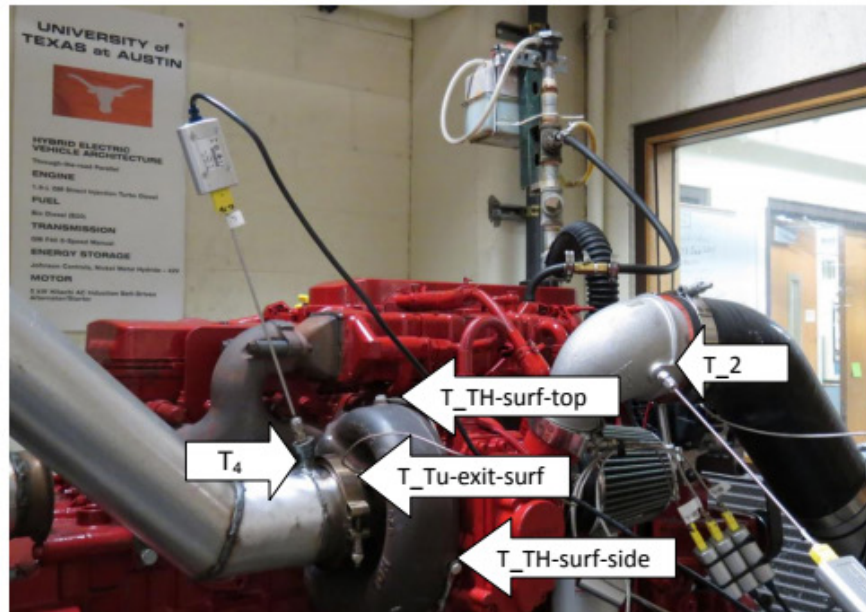
Figure 2-1   Temperature measurements around the turbocharger.

As labelled in Figure 2-1, we measured the temperatures at a location on top of the turbine housing surface (*T_TH-surf-top)*, the surface temperature on the side of the turbine housing (*T_TH-surf-side)*, and the surface temperature of the exhaust pipe right at the turbine exit (*T_Tu-exit-surf)*. *T_2* provides the charge air temperature after the compressor but before it enters the charge air intercooler and T_4 (*T_4)* is for the exhaust gas temperature directly downstream from the turbine exit. Furthermore, there are thermocouples installed to measure the temperature of the exhaust flow before it enters the turbine as well as the temperature of the engine oil as it leaves the turbocharger center section; these are called T_3 and *T_TC-exit-Oil*, respectively.

As seen in Figure 2-2, the temperature probes were installed such that the PTP turbo blanket can be installed in the same way as without the sensors underneath. This helped to keep from influencing the values to be measured by the method chosen (good surface contact is crucial; all surface sensors are bolt-on type), and this is also to ensure realistic

temperature measurements without any alteration of the insulation effect of the blanket (no increased gaps between blanket and turbine housing wall).

Figure 2-2   Unchanged tight fit of the PTP turbo blanket with temperature probes underneath it.

A humidity probe was mounted at the inlet of the air filter. It provided accurate readings of the air temperature and humidity and completes the set of measurements done externally.

2.2 Experiments and Data

For all runs the ECM settings were not changed between the baseline and the operation with a turbo blanket installed around the turbine. The test results were statistically evaluated because engine tests are not precisely repeatable.

Intake air boosting of an internal combustion engine can be realized with different devices. In the case of an exhaust gas turbocharger the coupling to the engine is done thermodynamically. Thus, the engine and booster can be evaluated separately. The

recorded data was first analyzed with respect to the performance of the turbocharger alone. However, not only for the vehicle operator but also for research purposes the performance of the entire system is relevant. Therefore, we will also evaluate the engine torque which is the critical parameter to look at for better acceleration.
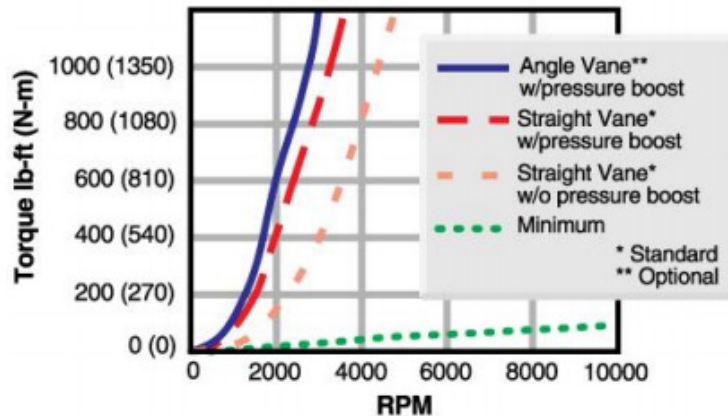

Figure 2-3 Dynamometer absorption curves. Our setup corresponds to the curve labeled straight vane with pressure boost.

The first test was a series of steady-state measurements at different engine speeds. Due to the limits imposed by the dyno (Figure 2-3), we needed to start with a relatively low torque for the low-speed point. The operating conditions of the following speeds were chosen so that the boost parameters increased in a linear fashion. We arranged the thermocouple wiring such that we were able to mount the TB while the engine was running in a certain operating condition which enabled us to conduct back-to-back measurements, thereby creating a real blanket vs. no blanket comparison because no additional uncertainties were introduced. This provided the best comparability possible. Repeatability is ensured in this case since the dyno controls are left without a single human intervention which, in turn, also saves time since cool-down and warm-up periods (the turbocharger used with this 6.7 L engine has relatively large dimensions if compared to turbo applications for passenger car engines, so the time it takes for heating or cooling is a significant factor) can be avoided. In combination with this, changing weather conditions (such as temperature, barometric pressure, relative humidity), that can occur within an hour period, can also cause

a significant change of the ambient condition inside the engine room if pre-conditioning is not available; this presented another strong argument for using back-to-back tests for better repeatability.

Three transient tests were performed. In the first two tests a load tip-in was executed while the dyno is in speed control mode. Two different speed-load points as the initial steady-state condition were chosen; these are 122 Nm (90 ft-lbf) at 1500 rpm and 136 Nm (100 ft-lbf) at 1750 rpm. By this approach we wanted to approximate the initial portion of a hard acceleration transient out of a cruising speed driving condition where the reaction of the engine speed via the acceleration of the vehicle is much slower as opposed to the almost instant increase of the load. Due to limitations of the dynamometer at 1500 and 1750 rpm we used the load tip-in and speed tip-in dyno control modes simultaneously to obtain another comparison. This methodology also brought us closest to transient scenarios experienced during hard accelerations performed with a vehicle on the road.

2.3 Statistical Relevance of Logged Data

Engine experiments are never precisely repeatable, primarily because the combustion process is not repeatable. Therefore, determining the statistical significance of the results is crucial. All steady-state operating conditions were conducted over a period of time such that the entire sample size is at least n = 600, in order to allow the following analysis. The mean values were calculated to obtain the standard error of the mean (also called the standard uncertainty of the mean), SEM:

$$SEM = 1.96 \frac{\sigma}{\sqrt{n}} \qquad (2.1)$$

where σ is the standard deviation of the data set, n is the number of data points in the data set, and the constant (1.96) yields the 95% confidence interval (*CI*). Specifically:

$$\frac{Upper}{Lower} 95\% \, CI = mean \frac{+SEM}{-SEM} \qquad (2.2)$$

When comparing two sets of data, if the confidence intervals do *not* overlap, one can say, with 95% statistical confidence, that the results are different. Conversely, if the

confidence intervals *do* overlap, one can say, with 95% statistical confidence, that there is *no* difference in the results.

One can apply this technique either to steady state data or to transient data, such as the present tip-in transients. However, in the case of transient data this technique can only be applied to a net result over the transient, such as the total fuel consumed.

The statistical approach for transients is different since values now change over time. We rather need a statistical evaluation of every individual reading along the time axis. To do this, we repeated a tip-in event multiple times and timed them with a stopwatch in order to obtain five events that have an equal duration of the transient as well as the settling time in between them. The turbine housing did not heat up severely during the short tip-in. However, in between them a certain amount of time (depending on the amount of heat transferred during the transients) had to elapse for the temperatures to settle back to their steady-state condition. This can certainly change significantly with the wall thickness of the turbine, i.e. the size of the turbocharger, so we used the turbine surface temperatures (*T_TH-surf-top* and *T_TH-surf-side)* as an indicator and started the next tip-in after they had dropped by about 2 °C, which can take several minutes. We thereby know that the temperature gradient across the entire turbine wall has changed the sign. And since heat transfer is a relatively slow process we assume that the internal surface temperature had approached the exhaust temperature in the turbine by the time the outer wall temperatures started to cool down again.

The entire data set was examined with regard to consistency of the heating and cooling periods, to ensure a quasi-steady-state characteristic over the course of six to eight individual tip-ins. Then, five events with consistent characteristics were picked and aligned using several engine and boost parameters to exactly match the beginning of the transient phase. As a result, we obtained a valid ensemble to create averaged tip-in curves as they are presented in Sec. 3.2. Therefore, for every test and in each case, i.e., with and without turbo blanket, five individual transients were aligned. In the case of the simultaneous tip-in we used a parameter called *accelerator pedal position* (Figure 2-4) which provided the most accurate technique for time-alignment here since two tip-in modes (speed and load tip-in) had to be triggered simultaneously. Note that the accelerator pedal position is a parameter calculated by the ECU to calculate the fueling according to a set of input parameters that also take intake properties into account. Hence, we obtain a curve with different slopes between turbo blanket and baseline operation. The onset of the acceleration is yet always

the same since it marks the reaction to the tip-in switch which makes this parameter perfect for alignment purposes in the post-processing.
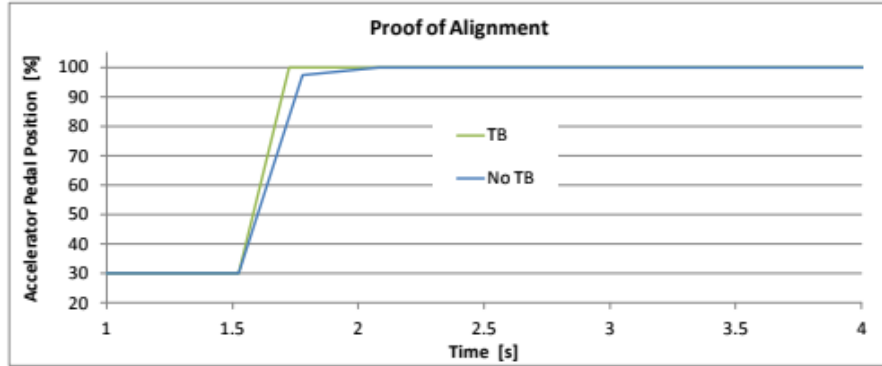
Figure 2-4   Alignment of the transient case with simultanuous tip-ins. Both curves depict the mean of five individual tip-in events each.

All of the logged data acquired during the present experiments were statistically analyzed.

2.4   Corrections to SAE Standards

Because Diesel engines are not throttled, the thermodynamic state of the intake air and of the fuel must be corrected to "standard" conditions. The correction factor for Diesel engines is prescribed for the brake power by SAE Standard J1349:

$$bp^c = bp^m (CF_a)^{f_m} CF_f \qquad (2.3)$$

A similar equation for correcting the torque is not specified but one can be generated:

$$(2\pi\tau N)^c = (2\pi\tau N)^m (CF_a)^{f_m} CF_f$$

$$\tau^c = \tau^c (CF_a)^{f_m} CF_f \qquad (2.4)$$

where the air correction factor is

$$CF_a = \left(\frac{99}{P_i^T - P_i^v}\right)^\alpha \left(\frac{T_i}{298}\right)^\beta \tag{2.5}$$

In Equation (2.5), T_i is the temperature of the fresh air entering the air filter in K, P_i^T is the barometric pressure, and P_i^v is the partial pressure of the moisture in the air. The partial pressure of water in the intake air stream is related to the relative humidity, Ω, via:

$$P^v = \frac{\Omega}{100} P_{sat} \tag{2.6}$$

where P_{sat} is the saturation pressure at the temperature of the inlet air, which can be obtained from:

$$\log(P_{sat}) = 6.77405 - 1.31797 \cdot 10^3 \left(\frac{1}{T}\right) - 2.0102 \cdot 10^5 \left(\frac{1}{T}\right)^2 + 1.08245 \cdot 10^7 \left(\frac{1}{T}\right)^3 \tag{2.7}$$

where the temperature must be in K, yielding the saturation pressure in kPa.

The exponents required for use in Equation (2.5) are also specified by SAE Standard J1349. For turbocharged engines without an intercooler (charge air cooler) or with an air-to-air intercooler such as the 6.7 L Cummins turbodiesel has, $\alpha = 0.7$ and $\beta = 1.2$. The exponent in Equation (2.3), f_m, is called the mechanical engine factor and is calculated using:

$$f_m = 0.3 \qquad\qquad \text{if } \frac{q}{r_p} < 37.2 \text{ mg/L} \tag{2.8}$$

$$f_m = 0.036 \left(\frac{q}{r_p}\right) - 1.14 \qquad\qquad \text{if } 37.2 < \frac{q}{r_p} < 65 \text{ mg/L} \tag{2.9}$$

$$f_m = 1.2 \qquad\qquad \text{if } \frac{q}{r_p} > 65 \text{ mg/L} \tag{2.10}$$

where

$$q = \frac{10^3}{60} \frac{\dot{m}_F}{D(N/x)} \text{ [mg/L]} \tag{2.11}$$

In Equations (2.8)-(2.10), the intake pressure ratio, r_p, is defined by:

$$r_P \equiv \frac{MAP}{P_i^T} \tag{2.12}$$

where *MAP* is the absolute pressure measured in the intake manifold and the denominator is the total pressure (including the partial pressure of the water - humidity) of the fresh air at the engine inlet. The Diesel also requires a correction for variations in the fuel density, Heating Value, and the fuel viscosity relative to standard reference conditions. These three properties are accounted for via two terms:

$$CF_f = f_d f_v \tag{2.13}$$

The first factor corrects for both density and Heating Value (energy density of the fuel):

$$f_d = 1 + 0.70 \frac{sg_{ref} - sg_{act}}{sg_{act}} = 1 + 0.70 \frac{0.850 - sg_{act}}{sg_{act}} \tag{2.14}$$

where 0.70 corrects for the variation of the Lower Heating Value via an empirical relationship between the specific gravity and the Lower Heating Value and 0.850 is the standard density of Diesel fuel in kg/L (SAE Standard J1349). The specific gravity of the actual Diesel fuel is to be determined at 15 °C.

$$\rho_f{}^{15.6\,C} = \rho_f{}^{T_f}(a + bT_f + cT_f{}^2) \tag{2.15}$$

where T_f is in °C and the coefficients depend upon the standard specific gravity and, for the ultra-low sulfur Diesel fuel used for on-road vehicles, are a = 0.98626, b= 8.6875·10^{-4}, and c = 8.4745·10^{-7}. In order to determine the specific gravity of the fuel, $\rho_f{}^{T_f}$, we measured the fuel density for six temperatures between 15 and 45 °C and divided these values by the corresponding densities of water (the density of water is well known over a wide temperature range). With these six supporting points we computed a curve fit to obtain the intermediate specific gravity values by interpolation.

The viscosity effect is accounted for via:

$$f_v = \frac{1 + S/v_{act}}{1 + S/v_{ref}} = \frac{1 + S/v_{act}}{1 + S/2.6} \tag{2.16}$$

where the fuel's kinematic viscosity is to be determined at 40 °C in mm^2/s, 2.6 mm^2/s is the standard kinematic viscosity at 40 °C (the standard fuel inlet temperature in SAE Standard J1349), and S is the dimensionless viscosity sensitivity coefficient of the fuel. Values for S are to be determined by the engine manufacturer. An older version of SAE J1349 stated that if values for S were not available, the following were to be used: 0.15 for pump/line/nozzle systems and 0.0 for unit injectors. This statement is absent in the Sept. 2011 version of this standard. The value for S was used as provided by the engine manufacturer. SAE J1349 specifies that the fuel inlet temperature must be between 39 and 41 °C for pump/line/nozzle systems and for common rail systems (such as used on the Cummins 6.7 L turbodiesel) and in the range 37-43 °C for unit injectors.

According to SAE Standard J1349, "The magnitude of the power correction for tests run at non-standard conditions should not exceed 3% for inlet air or 3% for inlet fuel corrections. If the correction factor exceeds these values, it shall be noted as a nonstandard test."

Because the Diesel requires the above correction for fuel properties, the specific fuel consumption is corrected in a different manner than is the case for the SI engine:

$$bsfc^c = \frac{\dot{m}_F{}^c}{bp^c} = \frac{\left(sg_{ref}/sg_{act}\right)f_v\dot{m}_F{}^m}{CF_af_df_vbp^m} = \frac{\left(sg_{ref}/sg_{act}\right)\dot{m}_F{}^m}{CF_af_dbp^m} \tag{2.17}$$

such that the viscosity term cancels.

To calculate the required correction factors, the humidity and air temperature were measured near the inlet to the air filter, the barometric pressure was extracted from the Cummins ECM, and the fuel temperature was measured using a thermocouple.

3 Results

3.1 Steady-State Operation

We first consider the turbocharger alone for our analysis since the thermal impact of the turbo blanket takes place on this device. Effects on the engine are a consequence of varying thermodynamic parameters due to the changed turbocharger performance. The PTP Turbo Blanket is an insulator, so we wanted to take a look at the temperatures first. Table 3-1 reflects the functionality of the applied TB well. Almost all temperatures have increased due to minimization of heat losses.

[°C]	T_2	T_3	T_TH-surf-top	T_TH-surf-side	T_Tu-exit-surf	T_TC-exit-Oil	T_4
No TB	93.2	535.7	307.8	258.1	366.8	105.4	462.6
TB	93.9	534.5	457.2	483.5	480.5	105.2	467.3

Table 3-1   Measured temperatures at 2250 rpm and 271 Nm (200 ft-lbf).

The insulation effect of the turbo blanket can be seen most obviously from the wall temperatures. In this case they increased by approx. 150 °C and 225 °C for the turbine top and the turbine side locations, respectively. Although not actually covered by the blanket, the wall surface temperature at the turbine exit is also tremendously increased which does not necessarily explain the higher exhaust gas temperature at the turbine exit ($\Delta T_4 = 4.7$ °C). This is the result of the energy saved during the expansion process through the turbine due to the better insulation on the outside of the turbine, i.e. the decreased heat flux through the turbine housing. The difference of the turbine inlet temperature T_3 is not significant for the discussion in this section and can be considered unchanged. But it can be seen from the values of the boost temperature at the compressor exit, T_2, that a portion of the recovered exhaust energy was also converted to physical work which was used by the compressor. As a result, effects can be seen on the cold side in terms of the boost pressure.

Higher boost pressures require that the compressor wheel spins faster. The following two plots in Figure 3-1 show these results for a series of low-load operating conditions (300, 300, 281, 258, and 246 Nm) at varying engine speeds (1500 – 2500 rpm); turbo speed values (left) are in units of 1000 rpm and the boost pressure on the right is a gage reading and in units of kilo-Pascals.
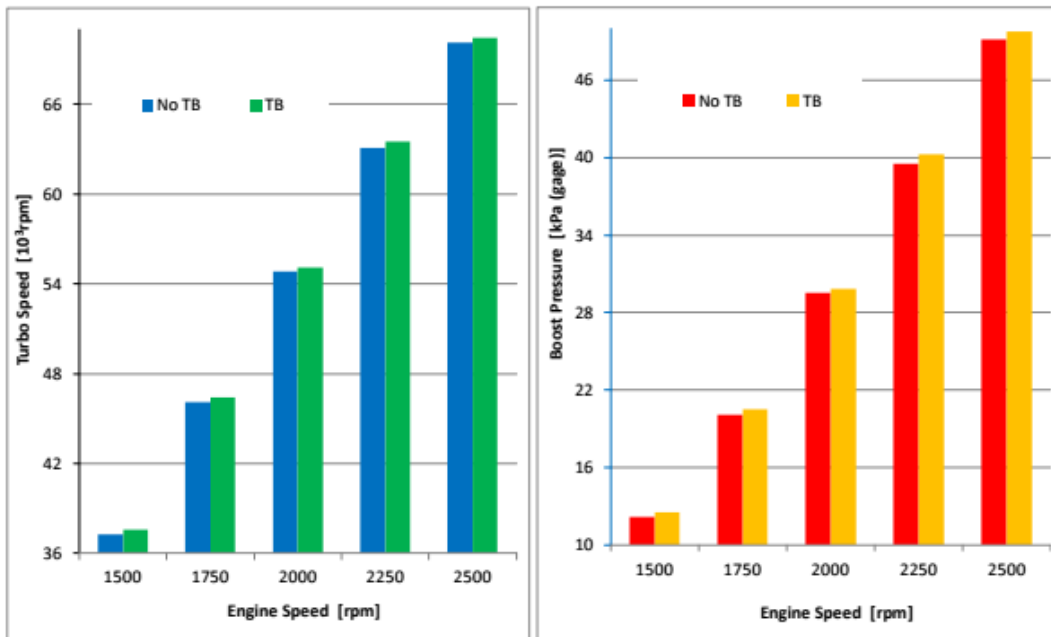
Figure 3-1 Comparison of the turbocharger shaft speed (left) and boost pressure (right) at five different steady-state operating conditions.

The torque levels of these speed-load points are approximately 25 – 30 % of the maximum engine torque. At such low loads the engine does not require high boost pressure; as we can see it is still below 50 kPa gage at 2500 rpm. Note that this Diesel engine is not equipped with an intake air throttle (compressor inlet pressure ≈ ambient pressure).

However, with the turbo blanket mounted, the turbo shaft speed exceeds the speeds of the baseline case for all of these steady-state operating conditions. The same trend is valid for the boost pressure which proves that more energy is converted to shaft work inside the turbine. Hence, this shows that even at a low load level, in which the turbine is not

provided with an excessive amount of exhaust waste heat, the increased boost performance is a direct result of the insulating effect of the PTP Turbo Blanket. These improvements are significant because if we consider, for example, that the remaining pressure drop across the throttle plate in a gasoline engine is on the order of roughly 2-3 kPa when in wide-open-throttle position, we can think of the turbo blanket as a way of effectively decreasing the flow resistance. Similar effects are reached by the use of improved air filter technology in an effort to increase the volumetric efficiency. For medium to high engine loads we expect more significant boost performance benefits. Hence, by operating the engine with a PTP Turbo Blanket we basically increase the volumetric efficiency across the entire map.

Also, if we consider these operating points in the TC compressor map, an increase of the turbo speed entails a shift toward higher compressor efficiencies even for the cases with high charge flow rates (2250 and 2500 rpm) – relevant for investigations to follow regarding the potential engine efficiency gain of a PTP Turbo Blanket.

3.2 Transient Response

3.2.1 Turbocharger Spool-up Comparison

In the prior subsection the benefit of the turbo blanket when the engine is operated in steady-state condition was examined. According to the theory, this was expected. We can see from the temperatures presented in Sec. 3.1 how much heat can be preserved within the turbine when a turbo blanket insulates the outer surface. From a thermodynamic standpoint it is clear that additional heat will be lost to the walls if the operating condition of the engine is changed to higher loads. The exhaust gas carries more energy out of the combustion chamber that can be expanded in the turbine. Now, from a heat transfer point of view, less heat will be conducted away from the housing walls during the expansion process because of the smaller temperature gradients in the case of turbo blanket operation. However, heat transfer is a slow process. Therefore, we want to know if the benefits of the turbo blanket are quantifiable during the relatively fast event of a hard acceleration transient. When the engine runs in low to medium-load steady-state condition (here: 1500 rpm, 122 Nm), which simulates a medium vehicle cruising speed, the load is suddenly increased to simulate a hard acceleration.

At the starting point and during the acceleration phase of this transient test the variable vanes of the VGT are mostly closed if the engine is operated in standard mode. This helps to increase the kinetic energy of the exhaust stream impinging on the turbine blades. The results of such a comparison between baseline and turbo blanket operation are less transferable to gasoline engines since almost all turbocharged gasoline engines do not use a variable geometry turbine. Therefore, we set the vanes to zero position so that they are completely open during the initial steady-state and the following transient acceleration. Moreover, the maximum engine output cannot be reached for the operating conditions presented below. Especially in the first case, the dyno absorption limit is still so low that the engine almost immediately runs into a "torque derate" mode which slows down the load increase rate to protect the dyno (as programmed into the Cummins ECM to allow operation using UT's SF-901 dyno). This effect shows up as prolonged curves that do not represent the actual engine performance in these points if the engine were in a vehicle rather than on a dyno.
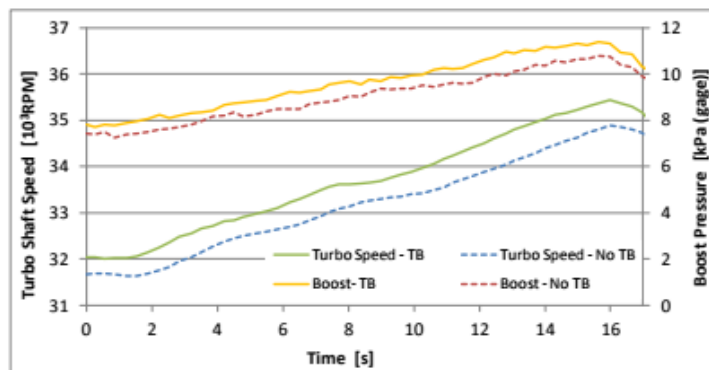

Figure 3-2   Boost pressure build-up on a load tip-in beginning at 1500 rpm and 122 Nm (90 ft-lbf).

In Figure 3-2 the turbo shaft speed and boost pressure are shown during such a tip-in event. The turbo speed was higher during the entire event when the turbo blanket was mounted. However, the slopes of the TB curves do not appear to be significantly steeper than those of the baseline engine/turbocharger. In this type of chart it cannot easily be detected that the turbo spool-up was faster and hence the boost pressure advanced more than at steady-state before the tip-in began. But we can see that, with the turbo blanket

installed, the turbocharger constantly delivered a pressure benefit of 1 - 1.2 kPa even though the engine output was derated and the fueling limited accordingly. The following section will show that the engine torque was significantly improved as a result of the effects shown in Figure 3-2.

Due to the dyno limitations we conducted another test with similar conditions (load tip-in at 1750 rpm and 136 Nm) in order to achieve higher boost levels (Figure 3-3). However, if this engine is used in a pickup truck, 1750 rpm would likely exceed any highway cruising speed. However, a brake torque of 136 Nm corresponds well to such a driving scenario, so one can think of it as a hard acceleration with a preceding downshift in order to overtake another vehicle.
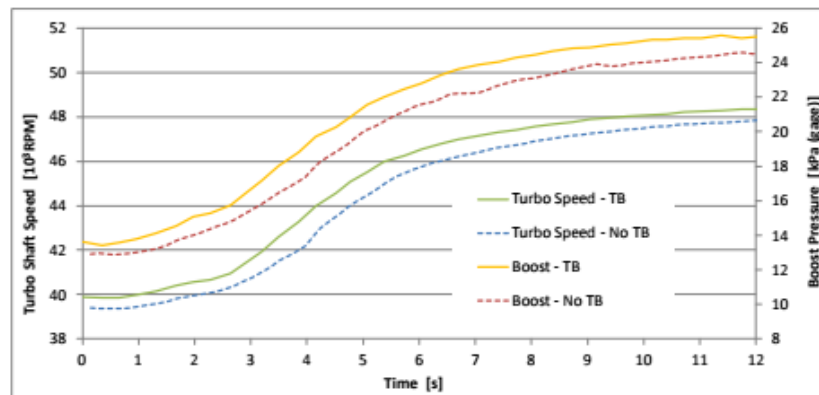

Figure 3-3   Load tip-in beginning at 1750 rpm and 136 Nm (100 ft-lbf).

When we begin the acceleration at a higher engine speed, the turbocharger speed is already noticeably higher. Since this Diesel engine is not equipped with an intake throttle (newer Diesels can be and gasoline engines always have a throttle) the turbo is required to deliver an increased amount of air which is almost linearly related to the engine speed. This, in turn, brings us closer to the maximum turbo speed which means that there is less inertia to overcome during the tip-in event. Thus, we expect to see a shorter duration for the spool-up and probably a decreased potential for benefits of a turbo blanket.

A comparison of the curve pairs in Figure 3-3 again shows that the compressor state has overall increased after the TB was mounted. For performance considerations it is, again, crucial how the boost pressure develops (yellow/TB vs. red curve/NoTB). In this plot

the tip-in switch took place at approx. 0.7 s. We notice that the boost pressure is already higher at this point with the turbo blanket, before the transient actually started. After about 3 s the yellow curve becomes noticeably steeper, thereby constantly increasing the pressure difference between baseline and turbo blanket operation. Note that these curves do not show a shift in the x-direction since they were aligned in time.
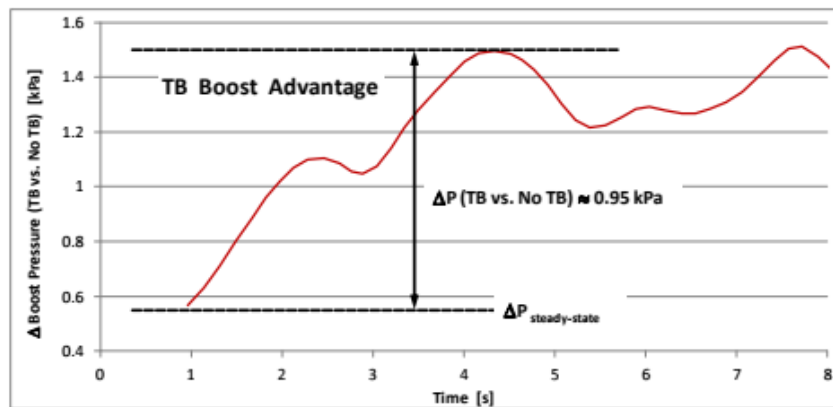

Figure 3-4 The pressure diffence (TB vs. No TB) history during a load tip-in beginning at 1750 rpm.

We are interested in how much more boost we were able to create with the turbo blanket at any given point during the transient. This is illustrated in Figure 3-4. The curve consists of values smoothened over four consecutive measurement points in order to better show the trend. The steady-state pressure difference was 0.55 - 0.6 kPa before the tip-in began. The trend in Figure 3-4 reveals the boost benefit gained with the PTP Turbo Blanket. The first data point at ~0.95 s was the average pressure difference ($\Delta P \approx 0.57$ kPa) approximately 0.25 s after the beginning of the tip-in with increasing values thereafter. Thus, the turbo blanket produced a boost advantage in less than 0.5 seconds. The curve peaks approximately 4 s into the tip-in event with a boost benefit of almost 1 kPa and continues to deliver a higher pressure – ΔP(TB vs. No TB) $\approx$ 0.65-0.95 kPa – for the next 4 seconds.

Overall, this might not seem to be a useful benefit at first glance, but if we consider these results in comparison with the following examples, we can better gauge the practical value. For performance (power and/or efficiency) purposes, one goal is to improve the

volumetric efficiency of an engine. The throttle plate inside the throttle body of a gasoline engine is still imposing a 2-3 kPa pressure drop on the intake air flow when the throttle is wide open, which cannot easily be decreased by a cost-efficient solution. Another idea is to lower the pressure drop of the intake air filter by using a different filter technology. Some aftermarket products are advertized to gain up to 2 kPa. However, such numbers are only valid for the highest air flow rates at wide open throttle operation. For part-load conditions the major pressure drop takes place inside the throttle body, thereby leaving much less potential for volumetric efficiency improvements via the air filter. In contrast to these examples, the PTP Turbo Blanket already demonstrated that it can provide a useful pressure gain over a much wider area of the engine map. These results will be much more pronounced when we take a look at the torque comparison in the subsequent section.

Due to the previously discussed dyno limitations at 1500 and 1750 rpm we used the load tip-in and speed tip-in dyno control modes simultaneously to obtain another comparison. This led to a relatively fast event, so that the first goal here was to find a speed and load range that allowed for a sufficient duration during which we did not have to operate near the dyno limits over the entire range. We found that we can switch both modes simultaneously if we start from the steady-state speed-load point of 81 Nm (60 ft-lbf) at 1000 rpm. As opposed to the first two transient cases the VGT was now controlled according to the VGT maps and control logic in the ECU. This methodology is comparable to a hard acceleration performed with a vehicle on the road. However, due to the lack of a transmission in between the engine-dyno setup to simulate a slower transient with a high gear ratio, this procedure is a relatively fast event and hence best compared to a hard acceleration in first gear on a level road.

Figure 3-5 shows the comparisons of the turbo shaft speed and the boost pressure. We first notice that the boost pressure lagged behind the turbo speed. A shorter time period available for a much wider load sweep (in comparison to the previously shown transients) results in much steeper gradients which pronounce the differences much more in this chart. However, the boost pressure started to increase only 0.25 - 0.30 s after the turbo speed started to pick up speed. Furthermore, it must be noted that turbo speeds and boost pressures matched closely before the tip-in began. The reason for that is the low steady-state load. Low-load operating conditions produce relatively small boost pressures. Especially at this low engine speed of 1000 rpm (idle: 700 rpm) it did neither result in a significant turbo speed advance nor in a boost pressure difference for the steady-state

condition between operation with the turbo blanket and baseline operation. Hence, we can read the differences of both variables for the following tip-in scenario directly from Figure 3-5.
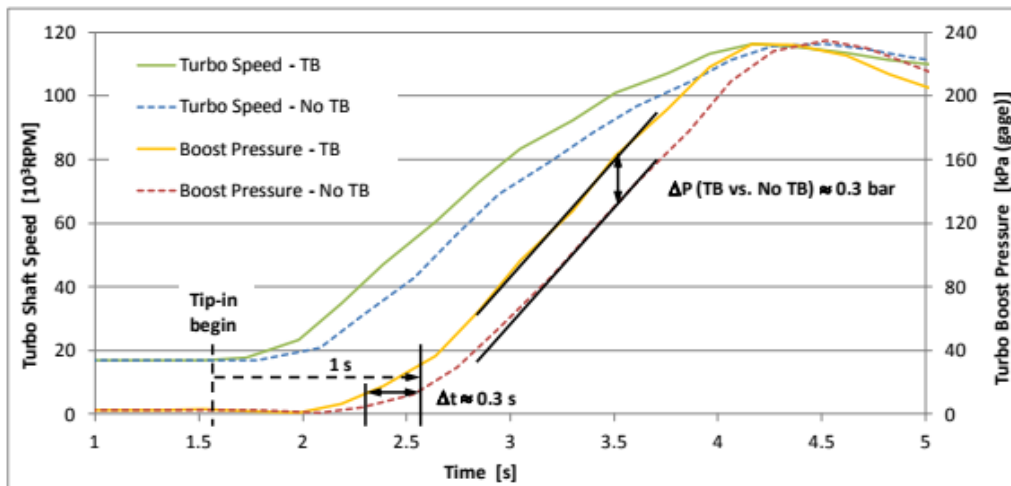

Figure 3-5   Load tip-in beginning at 1000 rpm and 81 Nm (60 ft-lbf).

The turbine/compressor speed advantage with the turbo blanket occurred right after the beginning of the tip-in and was as high as 10,000-12,000 rpm after approximately 0.5 s. The wide load sweep (from ~10% to 100%) in this comparison led to a considerably higher pressure difference between operation with the turbo blanket and the baseline case in comparison to the other two transient tests. After one second into the event of the baseline engine the application of the PTP Turbo Blanket led to a boost advance of about 0.3 s for this type of tip-in. This time advantage was followed by a boost pressure benefit of up to 30 kPa (= 0.3 bar) for the most of the engine acceleration so that the peak boost pressure was reached significantly earlier with the turbo blanket.

The results presented in this section demonstrate well that the PTP Turbo Blanket has a considerable impact on the turbocharger behavior and the thermodynamic properties of the intake air. But parameters such as the boost pressure are not something a driver can "feel" directly. The road performance benefit of the turbo blanket is important from an R&D perspective as well as from the driver's point of view. Therefore, we examined the brake

torque behavior of the engine because of its direct relation to the motive force between tire and road and, thereby, on the acceleration of the vehicle.

3.2.2 Time-to-Torque Comparison

In the previous section was shown that a thermodynamic advantage was obtained via the elevated state of the turbocharger when the turbine was insulated with the PTP Turbo Blanket. Those measures are tangible and very relevant from a R&D point of view. However, we also want to know if the engine output was affected. Did the time-to-torque performance improve and if so, by how much? Or in other words: will the driver be able to feel the "extra-boost"?
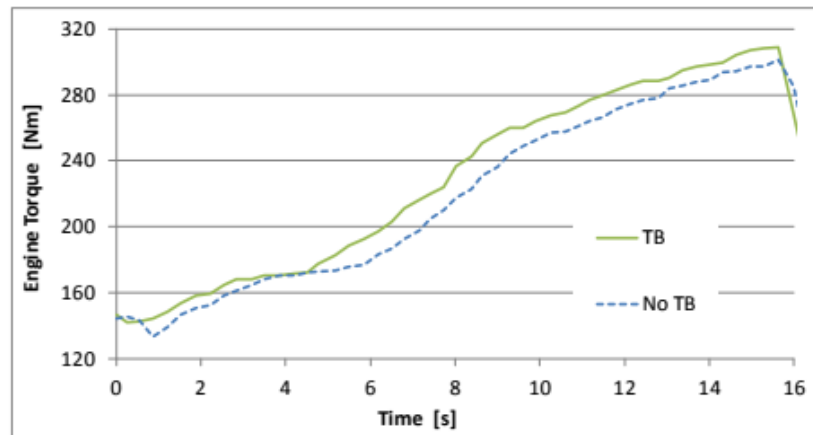

Figure 3-6 Comparison of the engine-dyno transient torque response on a load tip-in scenario at 1500 rpm.

The torque characteristic of the tip-in scenario at 1500 rpm – as discussed in Subsection 3.2.1 – is depicted in Figure 3-6. As described in Subsection 2.2, both curves were created from average values out of five individual measurements for each case: with and without the turbo blanket. We notice an initial drop of the baseline engine torque. If it would have occurred during one out of five measurements it would have disappeared after the averaging process. Further investigation is needed to find the cause for this behavior, but in this direct comparison it is the first advantage noticeable for the case in which the turbo blanket was mounted. In the following, both curves show very similar behavior, e.g.

both have a plateau area at 170 Nm. However, the turbo blanket case reached all torque levels before the baseline engine which means that the brake torque value at any point of time into the tip-in event is increased with use of the turbo blanket.

After 5-6 s the PTP Turbo Blanket produced a 15-20 Nm benefit. This is a remarkable result which also shows how much difference a seemingly small boost benefit (as shown in the previous section) can make. From then on the trend as well as the torque difference continued almost unchanged. Most transient load or speed scenarios cannot be matched to on-the-road driving conditions without the capabilities of a modern transient dynamometer, one of which was not available for the present tests. The limitations of the presented case, however, can be thought of as a suddenly inclined road which was climbed with the accelerator pedal restricted to a certain position. Both together stretch the time-to-torque span for which the case with the PTP Turbo Blanket has a clear boost advantage, as was shown in Figure 3-2.
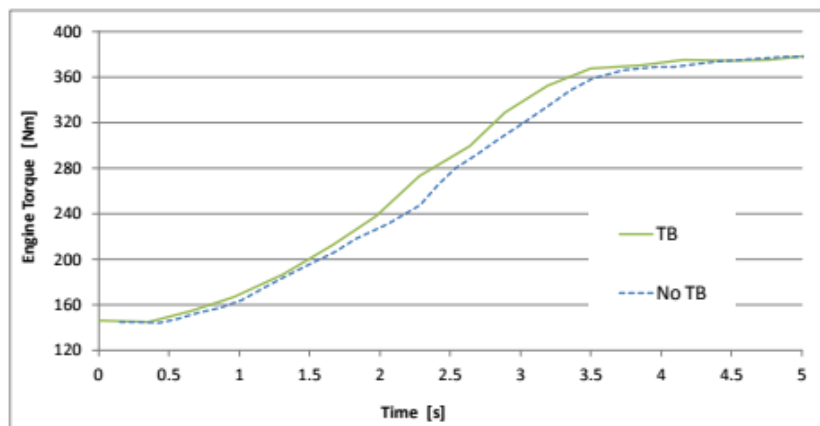
Figure 3-7   Comparison of the engine transient torque response (time-to-torque) at 1750 rpm.

In the case of the 1750 rpm load tip-in the whole event took place more rapidly than the one at 1500 rpm. Figure 3-7 illustrates, that the turbocharger benefit in the previous discussion (Figure 3-2 and Figure 3-3) was also true for the engine torque increase. Since this was a load tip-in, in which the engine speed was controlled to stay constant, the volumetric flow rate through the engine did not increase considerably. In addition to that, the

VGT was completely open (Sec. 3.2.1) throughout the whole acceleration. In general, these are reasons for a slower thermodynamic response of the system which can be seen at the beginning. Here, until about 200 Nm was reached, the difference between the baseline setup and turbo blanket operation was not significant. However, after a sufficient boost pressure benefit was provided by the operation with the PTP Turbo Blanket, the torque output also responded with a continuous advantage between 15 and 30 Nm until the dyno absorption limit was reached at ~375 Nm (Figure 3-7). Hence, we can now also confidently state that the seemingly small boost advantage presented in Figure 3-4 was crucial for the time-to-torque improvement of this transient case, even though it took place so quickly.
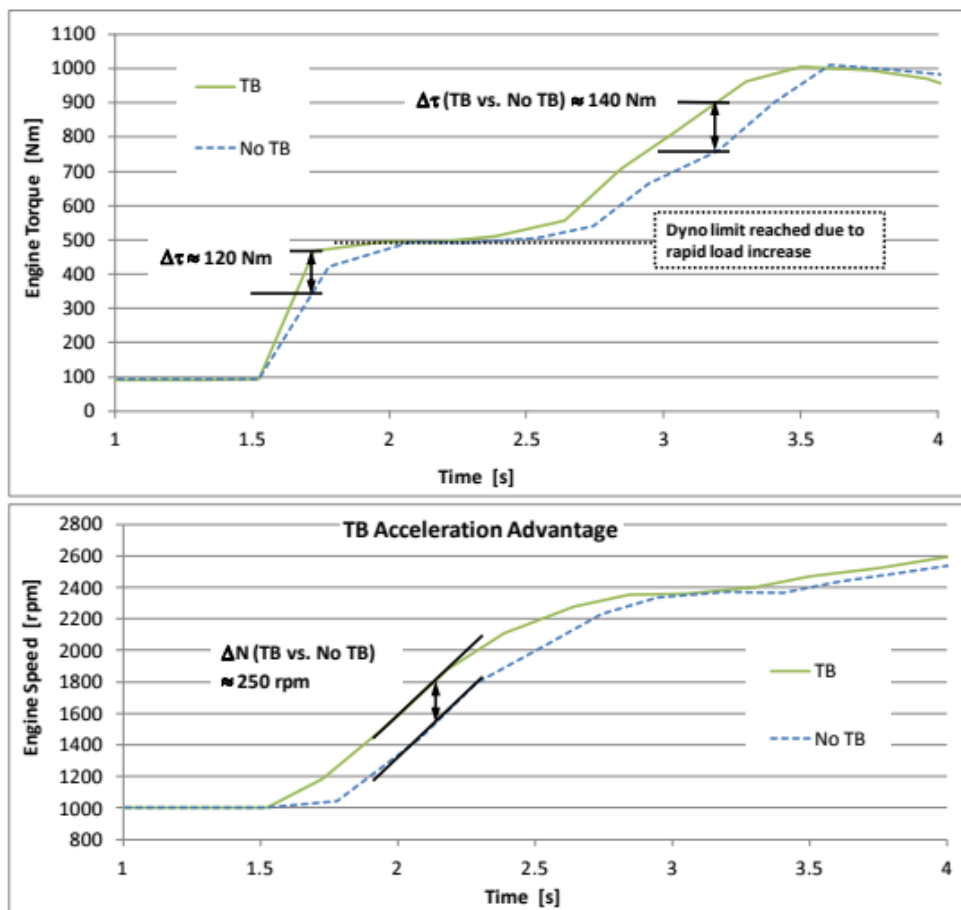
Figure 3-8   Comparison of the engine transient torque response at 1000 rpm. Top: Time-to-torque response. Bottom: Engine speed acceleration comparison.

Figure 3-8 shows a comparison of the engine responses on the simultaneous tip-in (see pg. 19 for tip-in conditions). The boost pressure built up faster than the acceleration of the system to a sufficiently high engine speed at which the dyno would have been able to absorb the instantaneous maximum torque output of the engine, which is why we obtained an approximately half second long torque plateau area (~500 Nm) as can be seen in the upper plot of Figure 3-8. However, when we conducted the test with the PTP Turbo Blanket mounted, the torque approached the plateau significantly before the baseline setup did. Even though this process took only a few tenths of a second the torque advantage provided by the turbo blanket was as high as 120 Nm in the meantime. Then, during the plateau phase, the two cases (turbo blanket vs. baseline) became leveled by the control system in terms of the torque output. However, the torque benefit of the turbo blanket also caused the engine to accelerate considerably faster. As the bottom chart in Figure 3-8 illustrates, the average engine speed was advanced by 200-250 rpm for the major portion of the engine acceleration (at 2350 rpm the control system reduced the acceleration rate as the engine's maximum speed was approached rapidly). Thus, the dyno restrictions were passed earlier with the TB applied to the turbo and the constant 0.2-0.3 bar boost pressure advantage (Figure 3-5) very quickly caused a torque benefit of up to 140 Nm until the rated torque of the engine was reached.

All three transient tests showed a significant engine torque advantage when the PTP Turbo Blanket was applied to the turbocharger. For the first two tip-in transients we increased the load instantly which is comparable to suddenly approaching hill with a constant gradient during which the driver steps on the accelerator pedal thereby increasing the load to 100%. The dyno limitations were not relevant for the function of the turbo blanket. Operation with the turbo blanket always benefited the turbocharger which, in turn, had a significantly positive impact with regard to the time-to-torque response of the engine. The third transient revealed intermediate torque advantages on the order of 140 Nm. However, there was still one dyno limit it had to pass before the torque continued to increase. Hence, according to the behavior shown in Figure 3-8, we assume that this advantage could be even bigger without the dyno limitations. We can find modern light-duty engines on the passenger car market that have a rated torque of 180 Nm delivered by a 1.2 L turbocharged Diesel. If we compare this number to the results we obtained by attaching the PTP Turbo Blanket to our 6.7 L Diesel engine, it was equivalent to an increase of the engine displacement on the order of 1 L with respect to the acceleration performance.

3.3 Further Observations

3.3.1 Relevance for Aftertreatment Technology

The previous sections showed that less heat is lost through the walls of the turbine housing with use of a turbo blanket. The data also revealed that a portion of the recovered energy was converted to shaft work since the turbocharger speed was increased for all turbo blanket cases. However, a certain amount of the recovered exhaust gas energy left the turbine as can be seen from the increased exhaust gas temperatures T_4.

T_4 [°C]	rpm	1500	1750	2000	2250	2500
No Turbo Blanket		413.1	436.3	447.4	462.6	469.8
Turbo Blanket		420.1	442.7	454.4	467.3	474.8

Table 3-2   Exhaust gas temperatures at turbine exit.

Table 3-2 lists the turbine exit temperatures for the following operating conditions: 300, 300, 281, 258, and 246 Nm at varying engine speeds from 1500 – 2500 rpm. Due to the insulation of the PTP Turbo Blanket the exhaust gas temperature downstream of the turbocharger was always higher in comparison to the baseline setup – ΔT_4(TB vs. No TB) $\approx$ 5-7 °C).

Note that for all operating conditions presented in this report the setup was not substantially changed. That is, the turbo blanket was applied to the turbine while everything else was kept to baseline conditions. Thermodynamically speaking, this is not the ideal solution for a turbocharged engine that is operated with a turbo blanket. For an integrated application, an even larger effect of the turbo blanket should be attainable if the design of the turbine is changed, if not the entire turbocharger design, in order to better use the recovered energy – a small part of which showed up as increased turbine exit temperature (T_4) – that would otherwise be lost for the turbine expansion process. In that way we expect an even better performance in terms of the power output of the engine.

Considerable efforts are made in order to reclaim energy from the hot exhaust gas which would otherwise be lost. Thermal management is a growing field in engines research

in which exhaust heat recovery (EHR) plays a significant role. The T_4 temperature difference caused by the application of the PTP Turbo Blanket is remarkable and is thus expected to become relevant not only for EHR but also for the purpose of pollutant emissions aftertreatment in the future.

3.3.2 Influence on Internal Oil Temperature of the Turbocharger

The measured turbine housing temperatures, as shown in Table 3-1, suggested that a significant amount of additional heat was induced on the hot side of the center section due to increased component temperatures when insulated with the turbo blanket. This raised the concern of potentially increased oil temperatures inside the turbocharger that can lead to something often referred to as oil coking or oil baking. For the steady-state operating conditions presented in Subsection 3.1 we also recorded the oil temperatures at the turbocharger center section exit.

T_TC-exit-Oil [°C]	rpm	1500	1750	2000	2250	2500
No Turbo Blanket		96.8	99.2	101.8	105.4	108.6
Turbo Blanket		97.0	99.4	101.8	105.2	108.8

Table 3-3   Comparison of measured temperatures of the engine oil leaving the turbo center section.

The values in Table 3-3 show that the heat impact on the turbocharger oil temperature was negligible. Modern turbochargers are well engineered devices involving a heat shield between the turbine wheel and the center section as well as separate cooling and lubrication circuits. Our measurements confirmed how well protected the bearings in modern turbochargers are. Even the considerably increased turbine housing temperatures (Table 3-1) during the operation with the PTP Turbo Blanket did not cause the center section oil temperature to rise by a significant amount. Thus, damage due to oil coking was not a concern during all our measurements.

3.3.3 VGT Internal Temperatures

The actuator for the variable geometry of the turbine inlet is located very near the hot wall of the turbine housing (Figure 3-9). For the operating conditions presented in

Subsection 3.1 we also logged the internal temperatures of the VGT actuator as they are also processed by the ECU.
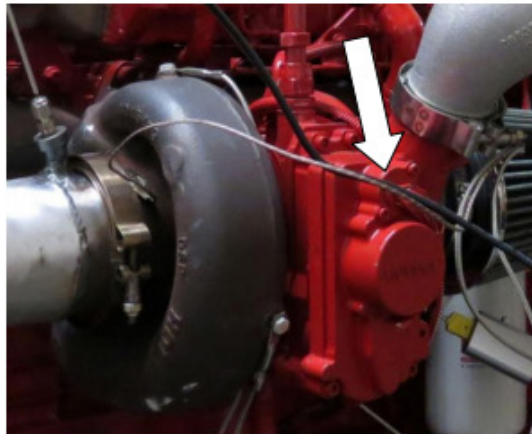

Figure 3-9   The VGT actuator (arrow) is directly attached to the center section.

VGT temp. [°C]	rpm	1500	1750	2000	2250	2500
No Turbo Blanket		79.0	80.0	81.0	84.0	86.7
Turbo Blanket		76.0	78.0	80.0	81.0	84.0

Table 3-4   Temperatures inside the VGT actuator.

Apparently, a significant heating process in the VGT actuator takes place due to the very nearby hot turbine. Temperatures as high as 80 °C (Table 3-4) inside the actuator can hardly be explained otherwise. The oil temperature did not considerably change between the baseline and the turbo blanket operation, as discussed in the previous subsection. Hence, we conclude that the temperature influence on the center section via heat conduction is minor, so heat conduction from the center section into the attached VGT actuator can also not be the cause for a major difference of the actuator's internal temperature. The ambient temperature in the engine room matched the temperature outside the building closely since the air was well circulated by the exhaust gas vents. However, from Table 3-4 we read a 1-3 °C decrease in the VGT actuator temperature when the turbo blanket is mounted. Thus, the other two heat transfer modes (convection and

radiation) between the turbine housing and the VGT housing must have been the main reasons for these temperature levels inside the actuator. The nearby sidewall of the turbine could not be insulated as well as most of the turbine housing because the gap was too narrow. Therefore, the turbo blanket contained less padding material in this location. However, the relatively small amount of PTP's padding that remained for this narrow gap insulated the turbine section well enough that the VGT actuator internal temperature dropped by up to 3 °C. This indicated that the PTP Turbo Blanket helped protect other engine parts against thermal damage, not only in the vicinity of the turbocharger but even helped to decrease the thermal load of a part that is directly attached to the turbocharger.

4 Conclusion

4.1 Summary

In this first report, we present experimental results concerning the performance potential of a baseline engine in comparison with the same setup when a PTP Turbo Blanket was applied to the turbocharger. We measured a series of steady-state cases to show how the turbo blanket affected the turbocharger operation. We then also set up different transient scenarios in order to evaluate the impact on the engine torque output. Furthermore, we discussed other observations to address further potentials of the PTP Turbo Blanket.

The application of the turbo blanket caused the turbine surface temperatures to increase significantly. This was expected and it is a necessity if a significant thermodynamic effect is sought. Without exception, all steady-state results proved this requirement for potential performance improvements. With the turbo blanket mounted, the turbocharger shaft speeds exceeded their baseline counterpart for identical engine operating conditions which resulted in increased boost pressures throughout all tested steady state speed-load points. However, since the engine-dyno controls tried to hold the system stable at the operating condition it was set to, we could not necessarily use this type of steady-state measurement to also test for the impact of the turbo blanket on the engine torque output.

Not only from a R&D perspective, but also from a vehicle operator point of view we wanted to know how much the improved steady-state boost results benefited in terms of the turbocharger shaft acceleration and, therefore, the advantage in boost pressure as well as the transient engine performance. In other words: will the turbo blanket provide a significant improvement with regard to the spool-up time of the turbocharger and will the vehicle acceleration be improved? Therefore, we compared the torque output by setting up three different hard acceleration transients.

The time-to-torque improvement with the PTP Turbo Blanket was significant, especially for the last case, in which we used a simultaneous tip-in of the speed and the load, the time-to-torque improvement was impressive with an instantaneous torque improvement of up to 140 Nm. This led to an acceleration advantage of 250 engine rpm in spite of the fact that the duration was less than 2.5 s for the entire event. The improvement

of the turbocharger performance provided this engine performance advantage because the turbocharger spool-up was faster which resulted in a boost pressure advantage of up to 0.3 bar when the PTP Turbo Blanket was mounted. Note that all three tip-in approaches were relatively fast events because they cannot be conducted differently with this type of engine-dyno setup. Thus, for vehicle transients, especially when operated in highest gear, we expect significant acceleration benefits with the turbo blanket.

We also observed phenomena that are noteworthy because they indicate further potential advantages of the PTP Turbo Blanket.

The temperature increase of the turbine housing was found to be significant which caused the exhaust gas temperature at the turbine exit to rise by about 5-7 °C. This was true for the tests as conducted; meaning no substantial change was made to the baseline engine setup. We merely applied the PTP Turbo Blanket to the turbocharger. For the case of an integrated application, for which the design of the turbine or the entire turbocharger would also be adapted accordingly, theory tells us that further improvements with respect to the torque performance are to be expected. The Engines Research Program at UT Austin is strongly interested in such endeavors but this requires the participation of a turbocharger manufacturer and/or an engine manufacturer.

In addition, higher exhaust temperatures downstream of the turbocharger can also be useful for any type of thermal management (particularly for exhaust heat recovery via, for example, an organic bottoming cycle) or aftertreatment device.

Since "oil coking" was a concern due to the significantly increased temperatures we measured on the turbine housing surface, we wanted to know if they affected the oil temperature in the turbocharger center section. The measurements showed a negligible influence. Hence, these results confirmed how well-engineered modern turbochargers are, so damage due to oil coking was not a concern during all our measurements.

From our readings of the VGT actuator internal temperature we can say that the PTP Turbo Blanket not only provides thermal protection for engine components in the vicinity of the turbocharger (such as electric/electronic components, hoses, wires, hydraulic lines, etc.) but it can even cause a temperature drop inside the actuator that is in direct contact with the center section of the turbocharger. Packaging is often a challenge in modern engine applications where little room is available to place auxiliary units and other devices. In such cases our measurements clearly indicated the potential of the PTP Turbo Blanket for improved thermal protection of very nearby parts.

4.2 Outlook

Our measurements showed that the key feature of the PTP Turbo Blanket was improvement of turbocharger performance and engine acceleration which will result in improved vehicle acceleration. At the same time, it provided a heat shield for nearby components while it did not significantly impact the heat conditions inside the center section of the turbocharger. The surface temperatures of the turbine housing were considerably increased and the exhaust gas temperature at the turbine exit increased somewhat. The increased turbine exit temperature with the turbo blanket could be beneficial with respect to waste heat recovery and emissions aftertreatment.

Advanced combustion modes with very high EGR rates have the potential for fuel consumption improvements of gasoline engines and will likely be seen in the near future. Combustion temperatures and hence the exhaust temperatures can drop significantly when the engine is operated with those combustion modes. This reduces the exhaust gas enthalpy which means that the time-to-torque performance of a turbocharged engine can be compromised below acceptable limits because the energy content of the exhaust gas is insufficient. The PTP Turbo Blanket can help to keep the turbocharger operation within acceptable limits when additional exhaust gas temperature is needed that would otherwise be lost during the turbine expansion process.

The requirements of future engines also include the sound emission from a turbocharger and its impact on the engine. During our measurements we were able to detect an audible difference between the operation with the PTP Turbo Blanket and the baseline engine setup. Hence, we will also make an attempt to evaluate the difference by performing sound pressure level measurements during our continued testing.

We will first follow-up with measurements on a vehicle dyno in order to obtain a better estimate of the presented results in terms of the transferability to vehicle performance.

Appendix

A. About the Authors

The Engines Research Program at The University of Texas at Austin has a long standing history. Dr. Ronald Matthews earned his Ph.D. in mechanical engineering from the University of California, Berkeley in 1977 and joined the faculty of The University of Texas at Austin in 1980, where he heads the General Motors Foundation Engines and Automotive Research Labs. In 1996 and again in 1998, UT's body of work on fractal engine modeling, led by Dr. Matthews, was nominated for the ComputerWorld Award and selected for inclusion in the Smithsonian's National Museum of American History Permanent Research Collection on Information, Technology, and Society. In 2002, he received four awards from the SAE: 1) he was elected to be an SAE Fellow, an honor bestowed to fewer than 20 people out of more than 100,000 society members each year; 2) he received the SAE's Excellence in Engineering Education (Triple E) Award, 3) along with former Ph.D. students and other faculty members he received the Myers Award for the most outstanding student-authored SAE technical paper, and 4) he was a recipient of the SAE Faculty Advisor Award. Dr. Matthews has been involved in engines research for over 35 years. In the early 1980s Dr. Matthews founded the Formula SAE Series[2], a collegiate competition in which students design race cars, and which has evolved since to become a worldwide competition today.

Steffen Bickle earned his Diplom-Ingenier degree in Mechanical Engineering from the Karlsruhe Institute of Technology in 2010, where he started to focus his studies on engines. He was involved in a "super knock" investigation in which he performed in-cylinder measurements of the local transient hydrocarbon content in the end gas. Since 2011, Steffen has been a graduate research assistant in the Engines Research Program at The University of Texas at Austin; here he gained knowledge in spark ignition modeling and – after a collaboration with the Advanced Combustion and Emissions group at the Southwest

---

Research Institute (SwRI, San Antonio) – turned his focus on the potential and challenges of future engines operating with new combustion modes in combination with advanced engine technology for highly boosted engines with extreme downsizing rates. Prior to his SwRI work he also gained knowledge and experience in turbocharging through several internships with IHI Charging Systems International, Heidelberg (Germany).

Steffen Bickle,
Graduate Research Assistant

Ronald D. Matthews,
Professor of Mechanical Engineering
Head: Engines and Automotive Research Program

Discover other performance fuel system parts on our website.